Hydrated Clusters of 2-Phenylethyl Alcohol and 2-Phenylethylamine: Structure, Bonding, and Rotation of the $S_1 \leftarrow S_0$ Electronic Transition Moment

Matthew R. Hockridge and Evan G. Robertson*

Physical and Theoretical Chemistry Laboratory, Oxford University, South Parks Road, Oxford, OX1 3QZ, U.K.

Received: January 4, 1999; In Final Form: March 3, 1999

Hydrated clusters of 2-phenylethyl alcohol (PEAL) and 2-phenylethylamine (PEA) have been studied in a jet-cooled environment, using laser-induced fluorescence excitation and mass-selected resonant two-photon ionization (R2PI) spectroscopy of the $S_1 \leftarrow S_0$ electronic transitions. Spectral features have been observed for clusters $M(H_2O)_n$, $n = 1-4$, and their stoichiometry assigned on the basis of the ion fragmentation patterns. Ionization of hydrated $PEA(H_2O)_n$ clusters leads to the observation of $PEA(H_2O)_{n-1}^+$ and $CH_2NH_2(H_2O)_n^+$ ions. Partially resolved rotational band contours of several $n = 1$, 2 clusters have been analyzed with the aid of ab initio molecular orbital calculations, conducted at the MP2/6-31G*//HF/6-31G* level for the ground state, and CIS/6-31G* for the first electronically excited singlet state. The analysis reveals the supramolecular structure: the host molecular conformation within these clusters and the binding sites of the water molecules. In $n = 1$ clusters of 2-phenylethylamine, the primary binding site involves hydrogen bonding to the nitrogen atom in the amine group. Cyclic hydrogen-bonded structures are observed for $n = 2$ clusters. In 2-phenylethyl alcohol, two different 1:1 clusters have been assigned in which the water molecule binds alternatively as a proton acceptor and proton donor. Further interactions between water molecules and the host, e.g., $H_{water}\cdots\pi$ and $O_{water}\cdots HC$, lead to additional stabilization of certain complexes. The assignments are aided greatly by the extraordinary sensitivity of the $S_1 \leftarrow S_0$ transition moment alignment to both side chain conformation and long-range intermolecular interactions.

1. Introduction

Supersonic jet spectroscopy provides an excellent means of isolating and identifying different conformers of flexible organic molecules and studying the structure and energetics of their solvated clusters.[1−16] Recent studies, conducted at very high resolution in Pratt's laboratory[1,2] and at lower resolution in our own,[3−7] have focused on rotational band structure for $S_1 \leftarrow S_0$ electronic transitions to assign conformers in a range of substituted aromatic molecules. The band contours are distinguished not only by inertial axis differences but also by strong, conformationally induced changes in the alignment of the $S_1 \leftarrow S_0$ transition moment (TM). Molecular orbital calculations, conducted at the HF/6-31G* and CIS/6-31G* levels have been remarkably successful at reproducing the experimental results.[3−7]

Questions of conformational choice have particular relevance to biological molecules, where secondary structure plays a crucial role in their functioning. In this context, the role of *intra*molecular hydrogen bonding and the consequences of solvation are very important. Many of the systems under current investigation either are biomolecules themselves or provide models for simple biological molecules. 2-Phenylethylamine (PEA) is the simplest member of a range of aromatic amine neurotransmitters and an analogue of the amino acid phenylalanine. The other related molecule, 2-phenylethyl alcohol (PEAL), is an important aroma component in various alcohol beverages.

The first LIF studies[8,10] of 2-phenylethylamine identified four separate origin bands that were assigned by Martinez et al.,[10] on the basis of power saturation measurements and relative spectral shifts, to two pairs of extended (anti) and folded (gauche) conformers, each split by alternative orientations of the terminal amino group. In subsequent microwave experiments, Godfrey et al.[11] were able to characterize the structures of the two gauche conformers **2** and **3**, shown in Figure 1, each of which appeared to be stabilized by hydrogen bonding to the π-electron system of the aromatic ring. Ab initio molecular orbital calculations conducted at levels of theory up to MP2/6-31G** supported these assignments but also predicted three other less stable conformers, one gauche and two anti.[11] Sun and Bernstein,[12] using a combination of LIF, mass-selected resonant two-photon ionization (R2PI), and hole-burning spectroscopy, found evidence for five origin bands. Four of these were assigned in a manner consistent with the earlier LIF and microwave studies, while the fifth and weakest band was thought to be associated with the "missing" gauche conformer predicted by the ab initio calculations.

Studying PEA at higher resolution, we obtained partially resolved band contours by LIF spectroscopy for each of the five origins in question, and the fifth peak was reassigned as a water cluster.[6] The other bands were assigned to conformers **2**−**5** of Figure 1. The anti conformers **4** and **5** display b-type rotational band contours, reflecting the L_b character of their first excited states. In contrast, the band contours of the gauche conformers display a hybrid character that reflects a strong rotation of the transition dipole moment in the molecular frame. We also used band contour analysis to assign molecular conformers of 2-phenylethyl alcohol. The most stable, conformer **2** in Figure 2, has a folded, gauche conformation of the side chain, which allows an intramolecular hydrogen bond between the terminal hydroxyl atom and the aromatic ring. The gauche conformers of 2-phenylethyl alcohol, like those of PEA, show hybrid band character, the extent of TM rotation depending

10.1021/jp9900077 CCC: $18.00
Published on Web 04/24/1999

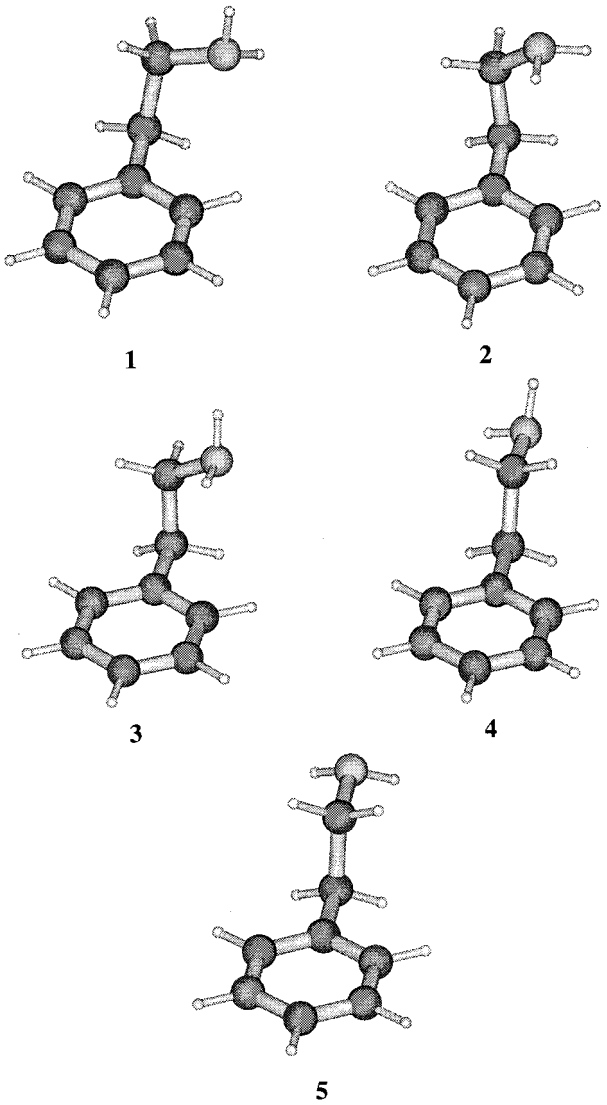

Figure 1. Conformers of 2-phenylethylamine predicted by MP2/6-311G** calculations.

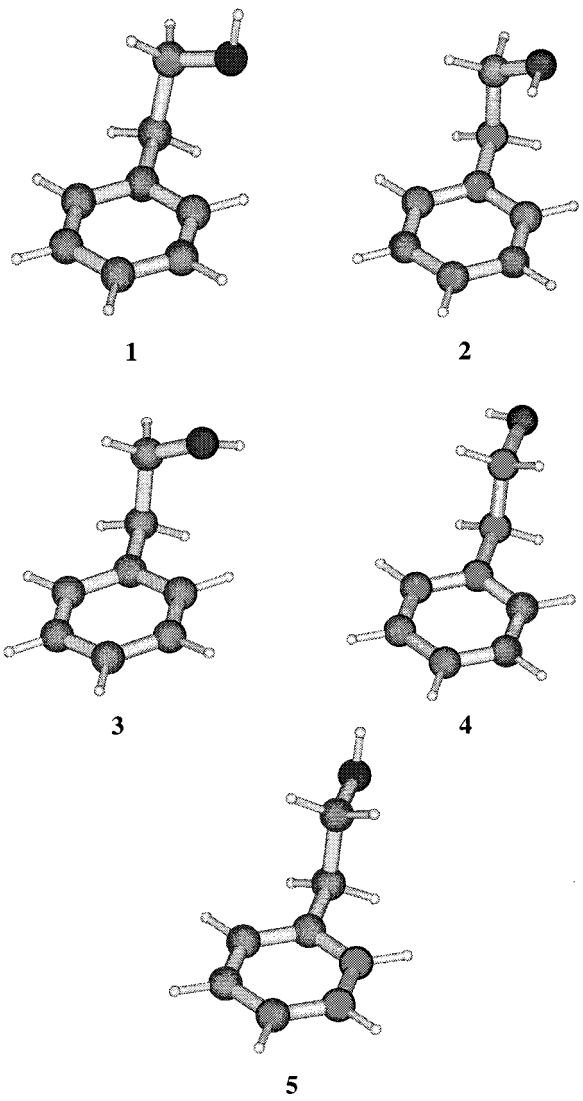

Figure 2. Conformers of 2-phenylethyl alcohol predicted by MP2/6-311G** calculations.

strongly on the orientation of the terminal hydroxyl or amino group. A related theoretical study found that the reorientation of $S_1 \leftarrow S_0$ TM alignments is associated with changes in the π-orbital composition, reflecting the influence of a "through-bond" effect caused by rotation of the substituent about the bond connecting it to the ring and a "through-space" effect, apparently caused by interactions of side chain orbitals with the π orbitals of the ring.[17]

The present paper describes new R2PI studies on hydrated clusters of 2-phenylethyl alcohol and 2-phenylethylamine. Spectral features are observed for clusters $M(H_2O)_n$, $n = 1-4$, and their stoichiometry is assigned on the basis of the ion fragmentation patterns. Partially resolved rotational band contours of several $n = 1$, 2 clusters have been analyzed with the aid of ab initio molecular orbital calculations to reveal the host molecular conformation, the binding sites of the water molecules, and the supramolecular structures.

2. Analytical and Experimental Procedures

2.1. Molecular Orbital Calculations. The possible binding sites of a water molecule to 2-phenylethylamine and 2-phenylethyl alcohol were explored initially, in the electronic ground state, by performing a series of ab initio molecular orbital calculations using Gaussian 94[18] using a 6-31G* basis set. The following procedures were pursued for a given molecular conformation.

(i) The geometry of the host molecule was set to its optimized structure in the absence of any solvent molecules. A set of structures was generated in which a water molecule was bound alternatively to hydrogen atoms or to "lone pair" sites on the side chain.

(ii) Each of these geometries was then submitted to full ab initio optimization at the HF/6-31G* level of theory. In cases where only one of the hydrogen atoms of the water molecule was bound to the host, the other hydrogen atom was rotated stepwise by 120° about the molecular OH axis and the resulting structure reoptimized to find any further local minima.

(iii) Force fields were calculated at the HF/6-31G* level for each optimized structure to ensure that they represented true potential minima and to obtain the zero-point energy corrections.

(iv) Basis set superposition errors (BSSE) were calculated to include the fragment relaxation energy:

$$E_{\mathrm{BSSE}} = E^{\alpha}_{\mathrm{AB}}(\mathrm{A}) - E^{\alpha\cup\beta}_{\mathrm{AB}}(\mathrm{A}) + E^{\beta}_{\mathrm{AB}}(\mathrm{B}) - E^{\alpha\cup\beta}_{\mathrm{AB}}(\mathrm{B}) \quad (1)$$

where $E^{\alpha\cup\beta}_{\mathrm{AB}}(\mathrm{A})$ is the electronic energy of fragment A in the geometry of the complex AB with the complex basis set $\alpha \cup \beta$.

TABLE 1: Molecular Parameters Predicted from MP2/6-31G*//HF/6-31G* and CIS/6-31G* Level Calculations of 1:1 PEA Water Clusters

	(PEA **1**)W_1	(PEA **2**)W_1	(PEA **3**)W_1(a)	(PEA **3**)W_1(b)	(PEA **4**)W_1	(PEA **5**)W_1
A''/MHz	1643.9	2565.4	1930.7	1699.4	2495.6	3127.7
B''/MHz	941.9	513.0	795.3	949.7	585.5	415.6
C''/MHz	777.5	508.5	638.0	797.0	502.2	408.6
A'/MHz	1538.5	2482.7	1900.8	1709.0	2445.9	3028.3
B'/MHz	951.9	512.6	788.1	935.5	581.6	413.4
C'/MHz	713.6	505.7	631.3	797.8	498.1	405.8
$\|R_e\| \times 10^{30}$/C m	1.40	1.15	1.27	1.87	0.98	0.97
μ_a^2:μ_b^2:μ_c^2	43:6:51	4:74:22	85:14:1	36:0:64	25:72:3	0:100:0
θ_{elec}, complex/deg	40	10	43	34	16	0
$\boldsymbol{\theta}_{elec}$, monomer/deg	34	10	22	22	2	0
ϕ_{elec}/deg	0	3	7	4	1	0
r(N···H−OH)/pm	213	207	206	(236)	207	209
E_{rel}/kJ mol^{-1} [a]	9.5	8.8	0.0	11.2	9.1	13.2
E_{bind}/kJ mol^{-1} [b]	23.2	20.3	23.7	14.5	21.1	19.6
E_{bind}/kJ mol^{-1} [c]	17.2	16.0	15.8	5.6	14.4	16.1
E_{bind}/kJ mol^{-1} [d]	30.1	25.7	30.8	18.5	27.0	24.7

[a] MP2/6-31G* + 0.9 × (zero-point correction)[†]. Corrections taken from HF/6-31G* calculations. [b] HF/6-31G* + 0.9 × (zero-point correction). [c] HF/6-31G* + 0.9 × (zero-point correction) + BSSE correction. [d] MP2/6-31G* + (0.9 × (zero-point correction) + HF BSSE correction). Corrections taken from HF/6-31G* calculations.

(v) MP2/6-31G* single-point calculations were performed using the HF/6-31G* optimized geometry.

(vi) The ground-state structures were subsequently optimized for the first electronically excited singlet state, at the CIS/6-31G* level of theory, to yield sets of rotational constants for the electronically excited S_1 state of each conformer, together with the magnitudes and directions of the $S_1 \leftarrow S_0$ TM.

A limited number of calculations were performed on cyclic, hydrogen-bonded structures of PEA$(H_2O)_2$ with the two most stable host conformations. Further calculations on 2-phenylethylamine clusters are described in the results and discussion sections.

2.2. Fluorescence Excitation Spectroscopy. Samples of 2-phenylethyl alcohol and 2-phenylethylamine were heated to temperatures in the range 70−100 °C and entrained in helium at stagnation pressures of 2−4 bar before their free jet expansion into a vacuum chamber through a pulsed nozzle valve (General Valve, series 9, 0.8 mm orifice) operating at 10 Hz. The expansion axis was intersected by a tunable UV laser beam at selected distances 2−12 mm from the nozzle aperture, allowing the spectrum to be recorded at different rotational temperatures. The fluorescence was collected along a third, mutually perpendicular axis. The laser source was a grating tuned, frequency-doubled dye laser (Lambda Physik FL3002) pumped by an excimer laser at 308 nm and operating at wavelengths of ca. 265 nm. An intracavity etalon provided a spectral line width of ca. 0.08 cm^{-1}. The LIF signals (detected by a photomultiplier through a 295 nm high-pass filter) and the excitation beam intensities (monitored by a photodiode) were both averaged using a boxcar integrator (Stanford SRS 250) and recorded on a PC.

2.3. Mass-Selected R2PI Spectroscopy. Samples of 2-phenylethyl alcohol and 2-phenylethylamine at 70−100 °C were entrained in helium at stagnation pressures of 3−5 bar. Water vapor could be incorporated into the gas stream by passing the helium through a water sample held in a bypass system at room temperature. The mixture was expanded through a pulsed nozzle valve (General Valve, series 9, 0.5 mm orifice) operating at 10 Hz into a vacuum chamber equipped with a differentially pumped time-of-flight mass spectrometer (R. M. Jordan). One-color R2PI spectra were recorded using a grating-tuned, frequency-doubled dye laser (Lambda Physik FL2002) pumped by a Nd:YAG laser at 355 nm. Two-color experiments were conducted using a second Nd:YAG-pumped (355 nm) and frequency-doubled dye laser (LAS LDL 20505) to provide the photoionization source. The two doubled dye laser beam outputs were combined coaxially to intersect the axis of the nozzle beam expansion but were separated by a time delay of ca. 100 ns to facilitate separation of the one- and two-color ionization signals. Photoionization signals were sampled using a digitizing oscilloscope (Tektronix TDS 520) and recorded on a PC as a function of laser wavelength and flight time.

3. Ab Initio Calculations

3.1. 2-Phenylethylamine. Optimized structures of 1:1 water clusters of PEA are shown in Figure 3, with molecular parameters summarized in Table 1. The arrows show the alignment of the TM in the molecular frame, described by the angle θ_{elec} (the angle between the short axis of the benzene ring perpendicular to the C_1-C_α bond and the TM). These structures include the most stable 1:1 water complex for each molecular conformer and an additional possibility for the most stable host conformation, PEA **3**.

The preferred binding site for the water molecule is, not surprisingly, the lone pair electron density of the amine group. Starting geometries that allowed for the alternative hydrogen-bonding scheme, with the water molecule binding as a Lewis base to the amino hydrogen atoms, did not converge unless a second H···π interaction "locked" the water molecule in place, e.g., (PEA **3**)W_1(b) in Figure 3d. The effect of other, weaker interactions may be seen in the position of the water molecule in (PEA **3**)W_1(a) and (PEA **4**)W_1; the second (non-hydrogen-bonded) hydrogen atom is directed away from the host molecule, and the oxygen atom is located ca. 2.7−2.8 Å from hydrogen atoms attached to either aromatic or aliphatic carbon atoms. A single MP2/6-31G** optimization was performed on the cluster (PEA **3**)W_1(a) to explore briefly the effect of adding dynamic electron correlation. The hydrogen bond length $r_{H\cdots N}$ was reduced from 2.06 to 1.94 Å, while the distance $r_{O\cdots H(ring)}$ was reduced from 2.75 to 2.44 Å, suggesting that both of these interactions are enhanced by adding dynamic electron correlation. Many of these trends are also observed in the binding energies of the different clusters. At the HF/6-31G* level, the complexes with the largest binding energies are (PEA **3**)W_1(a), in which the oxygen atom may interact with two host hydrogen atoms, (PEA **1**)W_1, where the water molecule is involved in an additional H···π bond, and (PEA **4**)W_1, with one additional weak O···HC interaction. When BSSE corrections are included,

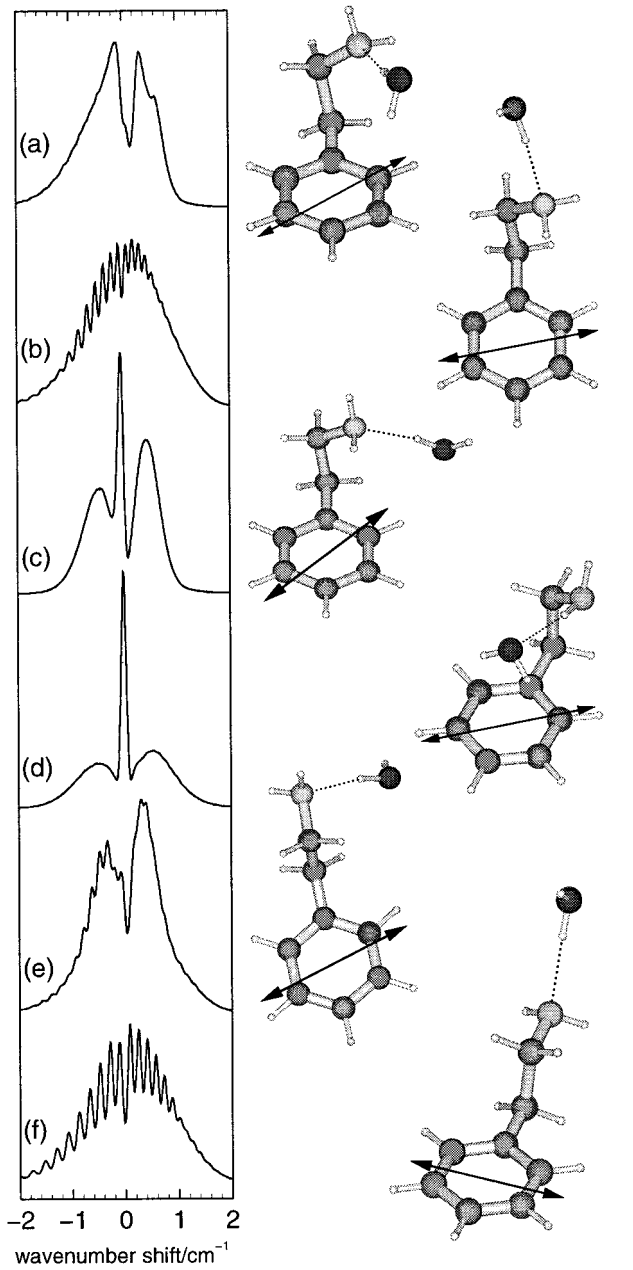

Figure 3. Simulated rotational band contours for the PEA(H_2O) complexes shown alongside the following, on the basis of the ab initio data detailed in Table 1 (T_{rot} = 4 K, laser line width = 0.1 cm^{-1}): (a) (PEA **1**)W_1, (b) (PEA **2**)W_1, (c) (PEA **3**)W_1(a), (d) (PEA **3**)W_1(b), (e) (PEA **4**)W_1, (f) (PEA **5**)W_1. The arrows show the CIS/6-31G* calculated $S_0 \leftarrow S_1$ TM alignments.

the binding energies of (PEA **3**)W_1(a) and (PEA **4**)W_1 are actually less than (PEA **2**)W_1 and (PEA **5**)W_1, a result that does not reflect the additional van der Waals interactions and is probably due to the incomplete basis set. The MP2/6-31G*// HF/6-31G* binding energies (including HF level BSSE corrections only) show larger differences, with the van der Waals interactions having a greater stabilizing effect. The magnitudes of the binding energies at this level are also more in line with more sophisticated calculations, for example, the value of 25 kJ mol^{-1} obtained for the NH···O bond in $CH_3NH_2(H_2O)$ at the LMP2/cc-pVTZ(-f) level by Marten et al.[19]

The 1:1 water clusters of PEA have widely varying rotational constants and $S_1 \leftarrow S_0$ TM alignments. As a result, their predicted band contours in Figure 3 show distinctive differences. The variation in θ_{elec} is similar to that observed for the monomer,

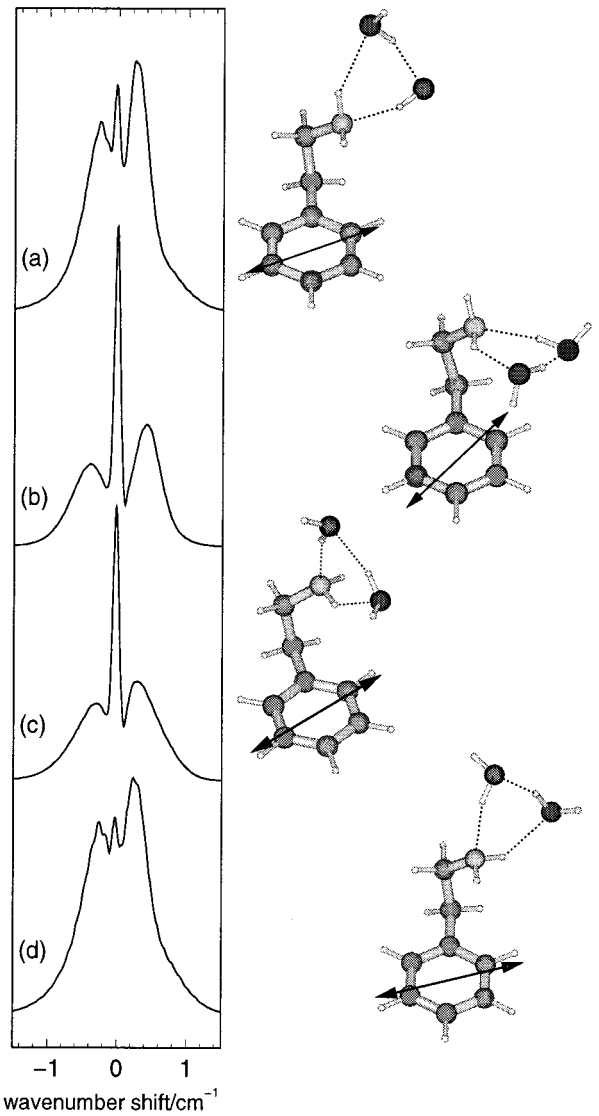

Figure 4. Simulated rotational band contours for the PEA$(H_2O)_2$ complexes shown alongside the following, on the basis of the ab initio data detailed in Table 2 (T_{rot} = 3 K, laser line width = 0.09 cm^{-1}): (a) (PEA **3**)W_2(a), (b) (PEA **3**)W_2(b), (c) (PEA **2**)W_2(a), (d) (PEA **2**)W_2(b). The arrows show the CIS/6-31G* calculated $S_0 \leftarrow S_1$ TM alignments.

but significant changes in θ_{elec} are also induced by the presence of the bound water molecule. Most notably, in (PEA **3**)W_1(a) the TM is rotated a further 21° from its alignment in the monomer (θ_{elec} = 22°).

A limited number of doubly hydrated structures were also calculated with the aim of finding the most stable ones to compare with experimental results. Only complexes of PEA **2** and PEA **3** were considered because intramolecular H···π bonding in these two conformers makes them considerably more stable than the others, a result confirmed by both theory and experiment.[6] The best configuration for two water molecules around the NH_2 functional group is a cyclic H-bonded network, similar in structure to the water trimer.[20] With one water bound at the favorable lone pair site of the nitrogen, there are two alternative amine hydrogens that may proton-donate to the second water to form a chain. This gives rise to the four possibilities shown in Figure 4, with molecular parameters summarized in Table 2. The most stable is (PEA **3**)W_2(b), which allows an additional H···π interaction. It also has the largest TM rotation, θ_{elec} = 52° according to the CIS/6-31G* calculation, perhaps due to the presence of a water molecule in

TABLE 2: Molecular Parameters Predicted from MP2/6-31G*//HF/6-31G* and CIS/6-31G* Level Calculations of 1:2 PEA Water Clusters

	(PEA **3**)W_2(a)	(PEA **3**)W_2(b)	(PEA **2**)W_2(a)	(PEA **2**)W_2(b)
A''/MHz	1806.4	1162.6	1264.1	1831.8
B''/MHz	390.1	742.2	544.1	383.7
C''/MHz	366.8	569.8	441.8	364.7
A'/MHz	1789.9	1164.9	1245.4	1817.5
B'/MHz	384.2	731.4	539.2	378.6
C'/MHz	362.1	558.9	438.9	360.8
$\|R_e\| \times 10^{30}$/C m	1.13	1.64	1.02	1.21
μ_a^2:μ_b^2:μ_c^2	44:48:8	72:1:27	28:3:69	31:66:3
θ_{elec}, complex/deg	21	52	21	17
$\boldsymbol{\theta}_{elec}$, monomer/deg	22	22	10	10
ϕ_{elec}/deg	6	2	5	4
r(N···H−OH)/pm	202	202	202	202
E_{rel}/kJ mol^{-1} [a]	6.6	0.0	10.7	5.4
E_{bind}/kJ mol^{-1} [b]	48.4	49.4	45.3	50.2
E_{bind}/kJ mol^{-1} [c]	35.1	31.0	32.5	37.4
E_{bind}/kJ mol^{-1} [d]	60.3	61.8	57.1	62.4

[a] MP2/6-31G* + 0.9 × (zero-point correction)[†]. Corrections taken from HF/6-31G* calculations. [b] HF/6-31G* + 0.9 × (zero-point correction). [c] HF/6-31G* + 0.9 × (zero-point correction) + BSSE correction. [d] MP2/6-31G* + (0.9 × (zero-point correction) + HF BSSE correction). Corrections taken from HF/6-31G* calculations.

TABLE 3: Molecular Parameters Predicted from MP2/6-31G*//HF/6-31G* and CIS/6-31G* Level Calculations of PEAL Water Clusters

	(PEAL **1**)w_1(a)	(PEAL **1**)w_1(b)	(PEAL **1**)w_1(c)	(PEAL **2**)w_1(a)	(PEAL **2**)w_1(b)	(PEAL **2**)w_1(c)
A''/MHz	1881.5	1782.9	2004.5	2001.3	1789.9	2796.3
B''/MHz	802.8	926.9	603.9	794.7	958.1	528.2
C''/MHz	625.3	807.2	543.3	642.1	821.6	501.4
A'/MHz	1824.1	1757.9	1964.2	1982.4	1821.2	2744.8
B'/MHz	809.6	911.9	596.1	779.3	940.5	522.3
C'/MHz	625.2	801.1	538.9	631.0	823.2	491.9
$\|R_e\| \times 10^{30}$/C m	1.32	0.89	1.02	1.02	1.83	1.11
μ_a^2:μ_b^2:μ_c^2	87:5:7	25:0:75	37:6:57	65:34:1	29:0:71	4:86:10
θ_{elec}, complex/deg	51	25	24	24	30	−5
$\boldsymbol{\theta}_{elec}$, monomer/deg	31	31	31	−4	−4	−4
ϕ_{elec}/deg	2	4	4	11	9	1
r(N···H−OH)/pm	201	213	200	200	202	201
E_{rel}/kJ mol^{-1} [a]	10.9	13.4	17.1	2.2	0.0	11.6
E_{bind}/kJ mol^{-1} [b]	18.3	19.1	18.3	21.0	21.2	16.7
E_{bind}/kJ mol^{-1} [c]	9.8	9.9	14.1	13.2	12.6	11.8
E_{bind}/kJ mol^{-1} [d]	21.5	23.3	22.2	25.9	27.4	19.5

[a] MP2/6-31G* + 0.9 × (zero-point correction)[†]. Corrections taken from HF/6-31G* calculations. [b] HF/6-31G* + 0.9 × (zero-point correction). [c] HF/6-31G* + 0.9 × (zero-point correction) + BSSE correction. [d] MP2/6-31G* + (0.9 × (zero-point correction) + HF BSSE correction). Corrections taken from HF/6-31G* calculations.

proximity to the aromatic ring. In (PEA **3**)W_2(a) where neither of the water molecules are close enough to affect the TM by through-space interactions, $\theta_{elec} = 21°$, almost identical to the value for the monomer.

3.2. 2-Phenylethyl Alcohol. Optimized structures of 1:1 complexes of PEAL are shown in Figure 5, and their molecular parameters are presented in Table 3. They are based only on the two most stable molecular conformers **1** and **2**, since the main focus of the calculations was to assist in the assignment of dominant spectral features. In each case, the water molecule may bind to the alcohol group as a proton acceptor or as a proton donor, with comparable binding energies. The strongest binding energy at the MP2/6-31G*//HF/6-31G* level is found for the cluster (PEAL **2**)W_1(b), in which the water molecule is situated above the ring, allowing H···π bonding similar to that found in (benzene)W_1.[13] The cluster with the next largest binding energy is (PEAL **2**)W_1(a), with the oxygen atom of the water molecule able to interact with a ring hydrogen atom in a fashion very similar to the phenylethylamine cluster (PEA **3**)W_1(a). These two complexes are more stable than their competitors by a considerable margin (ca. 9 kJ mol^{-1}), making it unlikely that increasing the basis set would displace them as the preferred clusters.

The placement of the water molecule in (PEAL **2**)W_1 clusters affects their rotational constants, their principal axis alignments, and their $S_1 \leftarrow S_0$ TM alignments to such an extent that the three band contours shown in spectra d−f of Figure 5 are quite different—one is predominantly a-type, one is b-type, and one is c-type. (PEAL **2**)W_1(a) and (PEAL **2**)W_1(b) both have TM rotations much greater than the corresponding molecular conformer PEAL **2**, but in (PEAL **2**)W_1(c), where the water molecule is far from the ring, θ_{elec} is almost unchanged.

4. Experimental Results

4.1. 2-Phenylethylamine Water Clusters. Mass-selected one- and two-color R2PI spectra of PEA and associated clusters in the $S_1 \leftarrow S_0$ band origin region are shown in Figure 6. Peaks A−D appearing in the PEA^+ mass channel have been assigned in our previous study to the structures PEA **5**, **2**, **3**, and **4** shown in Figure 1. The stoichiometry of the water cluster features is assigned by careful examination of their ion fragmentation patterns. First, we note that the parent ion is not observed in any of the PEA water clusters, and even with near-threshold ionization they lose at least one water molecule. This might be expected if the cluster undergoes a large geometry change upon ionization from S_1, as unfavorable Franck Condon factors may

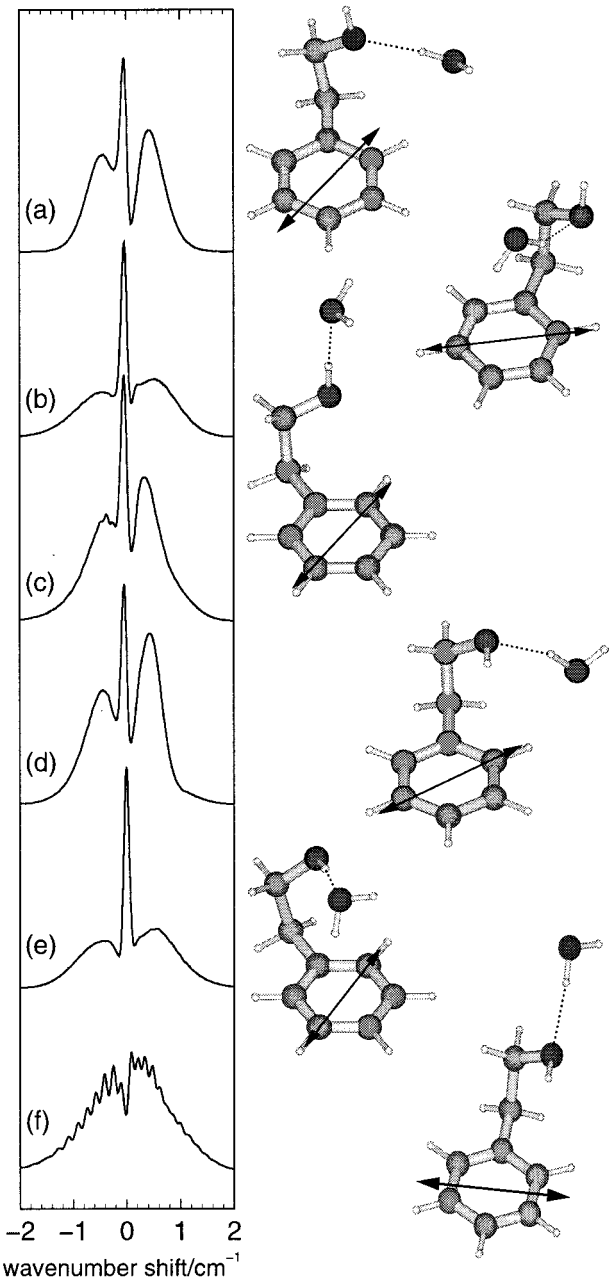

Figure 5. Simulated rotational band contours for the PEAL(H_2O) complexes shown alongside the following, on the basis of the ab initio data detailed in Table 2 (T_{rot} = 4 K, laser line width = 0.1 cm^{-1}): (a) (PEAL **1**)W_1(a), (b) (PEAL **1**)W_1(b), (c) (PEAL **1**)W_1(c), (d) (PEAL **2**)W_1(a), (e) (PEAL **2**)W_1(b), (f) (PEAL **2**)W_1(c).

rule out observation of the parent ion at the band origin. Notable examples are the benzene(H_2O)$_n$ complexes studied by Zwier et al.,[13] which undergo very efficient fragmentation. The hydrogen-bonded geometries that are most favorable for the neutral complexes are highly unfavorable repulsive geometries for the ionized complexes, since the positive hydrogens of water are directed toward the benzene cation. The unstructured nature of PEA photoelectron spectra[14] strongly suggests that the molecule itself undergoes a large change in geometry on ionization. This was interpreted as resulting from charge resonance and charge exchange interaction between the nearly isoenergetic electronic states associated with ionization of the phenyl and amine groups.[14] In support of this explanation, we find that HF/6-31G* optimizations of PEA ions give rise to structures in which the amine group is planar and carries a Mulliken charge of +0.5*e*. The geometry of neutral PEA(H_2O)$_n$ complexes, with a water molecule proton-donating to the nitrogen atom, would therefore be repulsive for the ionized complexes and lead to efficient fragmentation.

Although ionization of PEA water clusters does not lead to detection of parent cluster ions, an alternative fragmentation channel is observed that involves breaking the $C_\alpha-C_\beta$ bond to generate $CH_2NH_2^+$ ions bound to water molecules. The 1:1 water clusters for example appear in the mass channel 121, corresponding to PEA^+, and in channel 48, corresponding to fragment $CH_2NH_2{\cdot}H_2O^+$. This second fragmentation channel provides strong evidence that water molecules bind to PEA via the terminal amine group. Transition frequencies and observed ion fragmentation patterns for the water clusters are summarized in Table 4.

The details of host molecular conformation and water binding sites within the observed clusters have been further investigated through their rotational band contours. Spectra of the PEA(H_2O)$_n$ peaks labeled E, F, G, and H in Figure 6 have been recorded using LIF and two-color resonance-enhanced multiphoton ionization (REMPI) spectroscopy, and they are shown in the upper traces of Figure 7. Two-color ionization proved important in avoiding saturation and in preventing contamination of the peak G ion signal in mass channel 121 with the nearly coincident peak H ion signal in mass channel 139. The lower traces in Figure 7 are band contours that have been simulated using data from ab initio calculations at the HF/6-31G* and CIS/6-31G* levels. The corresponding structures that give rise to the simulated band contours are shown in Figures 3 and 4.

Excellent agreement between experiment and theory allows singly hydrated cluster peaks to be assigned with some confidence. The most intense 1:1 cluster feature, band E, is assigned to the structure (PEA **3**)W_1(a). In agreement with the CIS/6-31G* calculations for this structure, band E is predominantly a-type, in contrast to the corresponding monomer feature, band C, which is only 25% a-type.[6] This change reveals an enhanced TM rotation due to the presence of the water molecule, since inertial effects alone cannot account for it. Band G, the next most intense 1:1 feature, is assigned to (PEA **4**)W_1, which helps in turn to resolve some ambiguity in the previous assignments of the monomer bands A and D. These two bands have b-type contours with almost identical ^rQ and ^pQ subband spacing, which made it difficult to decide which was PEA **4** and which was PEA **5**. Band G, is blue-shifted by 26 cm^{-1} relative to band D, but by 116 cm^{-1} relative to peak A; this strongly supports the assignment of peak D to PEA **4**, since the equivalent shift in PEA **3** is only 23 cm^{-1}.

A further 1:1 cluster of similar spectral intensity observed at 37 596 cm^{-1}, blue-shifted from the monomer feature B by 37 cm^{-1}, is assigned to the structure (PEA **2**)W_1. It was not possible to obtain a band contour of this feature because there is so little signal in the $CH_2NH_2{\cdot}(H_2O)^+$ mass channel and the PEA^+ mass channel is congested from other peaks. The most likely candidate for the (PEA **5**)W_1 cluster is a weak feature at 37 591 cm^{-1}, blue-shifted 43 cm^{-1} from the monomer band A. The two remaining features in the $CH_2NH_2{\cdot}(H_2O)^+$ mass channel are blue-shifted by 4−5 cm^{-1} relative to bands E and G. They are also observed in mass channel 122, and the most likely assignment would be to species in which one of the ring carbon atoms is ^{13}C.

In both 3-phenylpropionic acid[3] and its *p*-hydroxy derivative,[9] 1:1 clusters are observed in which water binds as a proton acceptor to the acid group, red-shifted by ca. 10 cm^{-1} relative to the corresponding monomer feature. The observation of a series of blue-shifted satellite features appearing in the LIF

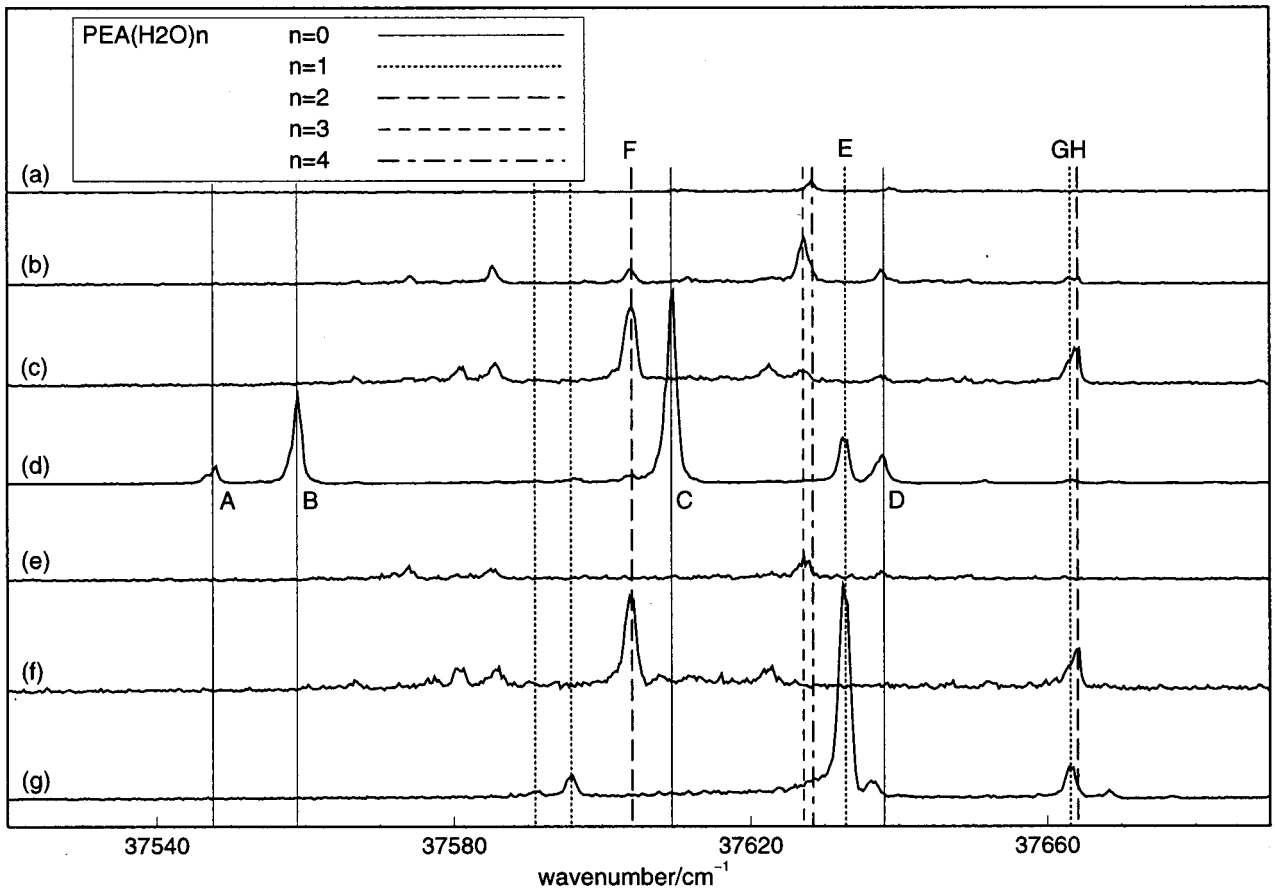

Figure 6. Mass-selected R2PI spectra of PEA and associated clusters in the $S_1 \leftarrow S_0$ origin region: (a) $m/z = 157$, one-color ionization; (b) $m/z = 139$, one-color ionization; (c) $m/z = 139$, two-color ionization ($\lambda_2 = 301$ nm); (d) $m/z = 121$, one-color ionization; (e) $m/z = 84$, two-color ionization ($\lambda_2 = 301$ nm); (f) $m/z = 66$, two-color ionization ($\lambda_2 = 301$ nm); (g) $m/z = 48$, one-color ionization.

TABLE 4: Ion Fragmentation Channels in Hydrated PEA Clusters

parent cluster	transition frequencies $\bar{\nu}$/cm^{-1}, 37610	obsd ions	
PEA	−62 (A), −51 (B), 0 (C), +26 (D)	PEA^+	$CH_2NH_2^+$
$PEA(H_2O)$	−14, +23 (E), +54 (G)	PEA^+	$[CH_2NH_2{\cdot}H_2O]^+$
$PEA(H_2O)_2$	−6 (F), +55 (H)	$PEA(H_2O)^+$	$[CH_2NH_2{\cdot}(H_2O)_2]^+$
$PEA(H_2O)_3$	+18	$PEA(H_2O)_2^+$, $PEA(H_2O)^+$	$[CH_2NH_2{\cdot}(H_2O)_3]^+$
$PEA(H_2O)_4$	+19	$PEA(H_2O)_3^+$, $PEA(H_2O)_2^+$	$[CH_2NH_2{\cdot}(H_2O)_4]^+$, $[CH_2NH_2{\cdot}(H_2O)_3]^+$

spectrum of PEA upon addition of water led Sipior et al.[8] to the conclusion that water was binding as a proton donor. The results of the present study confirm this finding, although their assignment of the molecular conformations was flawed.

The relative intensities of the water clusters associated with PEA conformers **5**, **2**, **3**, and **4** in the $CH_2NH_2{\cdot}(H_2O)^+$ mass channel, 3:11:100:15, are different from those of the corresponding monomer features A−D, 22:48:100:21. Bands E and G are enhanced compared to the other features, suggesting some additional stabilization of (PEA **3**)W_1(a) and (PEA **4**)W_1 if thermodynamic and not kinetic factors are responsible. The calculated binding energies of water to conformers **5**, **2**, **3**, and **4** at the MP2/6-31G*//HF/6-31G* level are 25, 26, 31, and 27 kJ mol^{-1}, respectively, in qualitative agreement with the observed trend.

Experimental contours of the 1:2 water cluster features F and H are shown in Figure 7, together with "ab initio" contours selected from the possibilities in Figure 4. The strongest feature, band F, has a contour that is best matched with the simulation based on (PEA **3**)W_2(b). The simulated contour of (PEA **2**)-W_2(a) is similar in appearance, but this structure is 11 kJ mol^{-1} less stable at the MP2/6-31G*// HF/6-31G* level. (PEA **3**)-W_2(b) is particularly stable because it allows for an additional H$\cdots\pi$ interaction. The contour of band H is quite similar to both the (PEA **3**)W_2(a) and (PEA **2**)W_2(b) simulations, although the height of the central Q-branch favors (PEA **3**)W_2(a) slightly. These two structures have very similar relative energies at the MP2/6-31G*//HF/6-31G* level, so their stabilities cannot be used as a criteria for assignment. The position of band H in the spectrum is a further consideration; it is blue-shifted by 55 cm^{-1} relative to band C (PEA **3**) and 106 cm^{-1} relative to band B (PEA **2**). The 1:1 clusters of PEA are blue-shifted by ca. 30 cm^{-1} from their corresponding monomer bands, which suggests that the 1:2 cluster band H is more likely to be associated with PEA **3**. The water molecules in both (PEA **3**)W_2(a) and (PEA **2**)W_2(b) are some distance from the ring, so a shift of 106 cm^{-1} would be surprising. Infrared spectral hole-burning experiments, which are planned for these systems, should provide more definitive assignments of these clusters and reveal more about the hydrogen bonding within them.

4.2. 2-Phenylethanol Water Clusters. R2PI spectra of PEAL and its hydrated clusters in the $S_1 \leftarrow S_0$ band origin region are shown in Figure 8. In contrast to PEA, parent ions of the PEAL-$(H_2O)_n$ clusters *are* observed, and the use of two-color near-

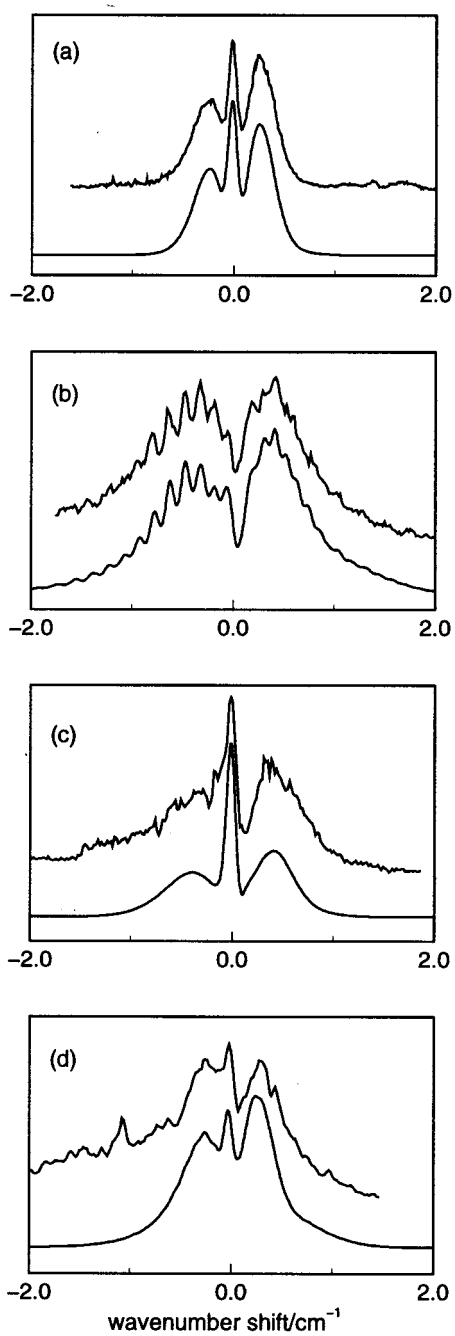

Figure 7. Rotational band contours of PEA. Upper traces are (a) LIF spectrum of band E and (b−d) two-color R2PI ($\lambda_2 = 301$ nm) spectra of bands G, F, and H. Lower traces are contour simulations based on ab initio data from Table 1: (a) (PEA **3**)$W_{1(a)}$, $T_{rot} = 1.2$ K, fwhm = 0.10 cm^{-1}; (b) (PEA **4**)W_1, $T_{rot} = 5$ K, fwhm = 0.08 cm^{-1}; (c) (PEA **3**)W_2(b), $T_{rot} = 3$ K, fwhm = 0.09 cm^{-1}; (d) (PEA **3**)W_2(a), $T_{rot} = 3$ K, fwhm = 0.09 cm^{-1}.

threshold ionization leads to very little fragmentation. Peak C* appears to show an ion signal in the PEAL$^+$ mass channel, but the band contours recorded in the PEAL$^+$ and PEAL$(H_2O)^+$ mass channels under two-color ionization conditions have very different appearances.[6] In our previous paper, band C was assigned to an anti conformer of PEAL and the overlapping band C* to a water cluster.

Band contours of the two most intense 1:1 cluster features, labeled C* and F, are shown in the upper traces of Figure 9. Ab initio values for the relative energies of PEAL water complexes quoted in Table 2 favor assignment of these two features to the structures (PEAL **2**)W_1(a) and (PEAL **2**)W_1(b).

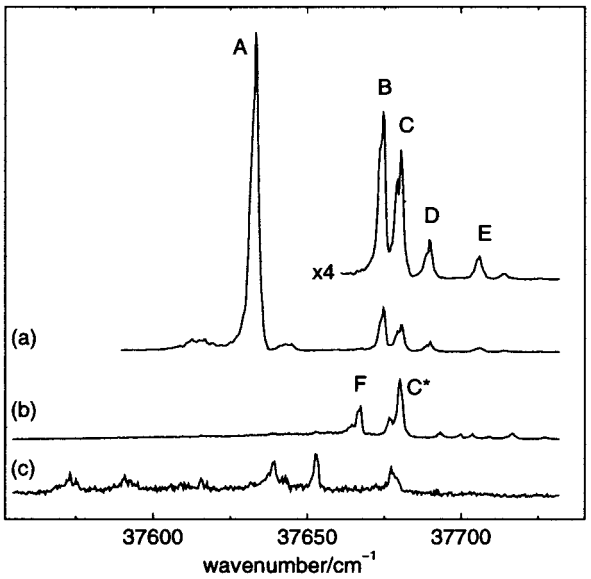

Figure 8. Mass-selected two-color R2PI spectra ($\lambda_2 = 288$ nm) of PEAL and associated clusters in the $S_1 \leftarrow S_0$ origin region: (a) m/z = 122; (b) m/z = 140; (c) m/z = 158, ×4.

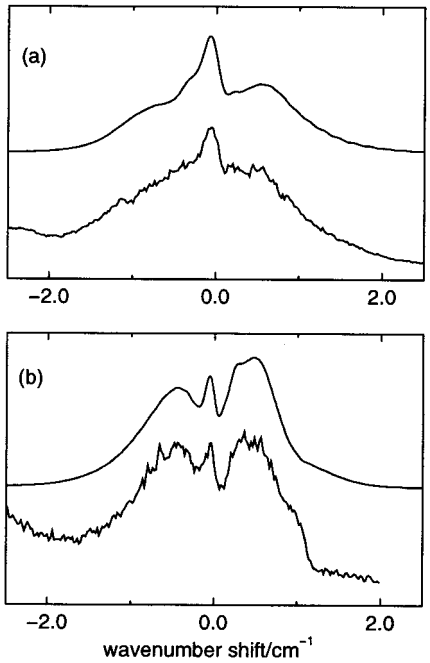

Figure 9. Rotational band contours of PEAL. Lower traces are two-color R2PI spectra of (a) band C* and (b) band F. Upper traces are contour simulations based on ab initio data from Table 2, with some modifications (see text): (a) (PEAL **2**)$W_{1(b)}$, $T_{rot} = 5$ K, fwhm = 0.12 cm^{-1}; (b) (PEAL **2**)$W_{1(a)}$, $T_{rot} = 5$ K, fwhm = 0.10 cm^{-1}.

They are ca. 10 kJ mol^{-1} more stable than the nearest competitors because the PEAL **2** host is so stable and because secondary interactions with the water molecule result in particularly strong binding energies.

The ab initio contours of Figure 5 are somewhat different from the experimental contours of bands C* and F, but with some minor modifications the simulated contours shown in the upper traces of Figure 9 can be generated. In Figure 9a, the excited-state rotational constants obtained from the CIS/6-31G* calculation of (PEAL **2**)W_1(b) have been altered, increasing A' by 0.002 cm^{-1} and decreasing C' by 0.001 cm^{-1}. These changes are not unique but illustrate that only small changes of geometry are necessary to produce a simulation very similar to the contour

of band C*. The error is most likely to arise from uncertainty in the position of the water molecule in this complex. The HF/6-31G* ground-state geometry has the water molecule bound to the aromatic ring via one hydrogen. In the CIS/6-31G* excited-state geometry both hydrogens of the water molecule are equidistant from the ring, but this changes to only one hydrogen if the basis set is increased to 6-31+G*. The next best candidate for band C* is (PEAL **1**)W_1(b), which places water over the ring in a fashion very similar to (PEAL **2**)W_1(b) and has a predicted contour that is almost identical. The MP2/6-31G*//HF/6-31G* calculations, however, favor (PEAL **2**)-W_1(b) by more than 13 kJ mol^{-1}, and on that basis, band C* is assigned to (PEAL **2**)W_1(b) rather than to (PEAL **1**)W_1(b). The simulation shown in Figure 9b above the spectrum of band F is based on the parameters from (PEAL **2**)W_1(a) but with the a:b:c type band character altered from 65:34:1 to 35:65:0, implying that θ_{elec} for the complex is only 8° rather than the 24° predicted by ab initio methods. Alternative assignments of band F to (PEAL **2**)W_1(c) or (PEAL **1**)W_1(a), the two remaining structures with predicted contours that are *not* predominantly c-type, would require even greater adjustment of θ_{elec} to produce the required hybrid band character. (PEAL **2**)W_1(c) is further ruled out because its rotational constants would result in visible subband structure, which is not observed. Calculated relative energies also lend support to the assignment of band F to (PEAL **2**)W_1-(a), since it is considerably more stable than either (PEAL **2**)-W_1(c) or (PEAL **1**)W_1(a) by a margin of ca. 9 kJ mol^{-1}.

The interesting finding is that two separate 1:1 clusters of PEAL **2** are observed, implying that there are two sites with comparable binding energies. The most intense 1:1 spectral feature, band C*, is assigned to the structure (PEAL **2**)W_1(b) in which water binds as both a proton acceptor to the alcohol group and as proton donor to the aromatic ring. The next strongest 1:1 feature, band F, is assigned to the structure (PEAL **2**)W_1(a) in which water binds primarily as a proton donor to the alcohol group but also to a ring hydrogen via the water's oxygen atom. The remaining features that appear only in the PEAL$(H_2O)^+$ mass channel, blue-shifted relative to bands C* and F, are tentatively assigned to 1:1 complexes in which the host PEAL molecule adopts different molecular conformations. It is likely that some of the other PEAL conformers also give rise to at least two 1:1 complexes, given the number of spectral features observed.

Finally, a number of peaks are observed in the PEAL$(H_2O)_2^+$ mass channel shown in Figure 8. The peak red-shifted by 3 cm^{-1} relative to C* fragments into the PEAL$(H_2O)^+$ mass channel, strongly suggesting that it is a 1:2 complex. The other features show very little fragmentation into the PEAL$(H_2O)^+$ channel, suggesting that they might arise from 1:3 complexes. It is expected that the most stable structure for a PEAL$(H_2O)_2$ complex would be one similar to (PEA **3**)W_2(b), benefiting from a cyclic hydrogen-bonded structure and an H$\cdots\pi$ interaction.

5. Discussion

Hydrated clusters of PEA and PEAL have been assigned first by examining their ion fragmentation patterns to determine the number of bound water molecules and second by comparison of their rotational band contours with ab initio predicted simulations to determine the details of host conformation and the disposition of the water molecules. In PEA, the first water molecule is hydrogen-bonded to the "lone pair" site on the amine group. A second water molecule can bind to form a cyclic hydrogen-bonded network with the amine group and the first water molecule. In PEAL, separate 1:1 clusters are observed in which the water molecule binds to the alcohol group alternatively as proton donor and as proton acceptor. In addition to these major findings, a number of other interesting results have emerged from this study.

The process of assigning cluster stoichiometry has been greatly assisted by the observation of $CH_2NH_2{\cdot}(H_2O)_n^+$ ions. Water molecules are retained by the $CH_2NH_2{\cdot}(H_2O)_n^+$ ions following scission of the $C_\alpha-C_\beta$ bond, while the PEA$(H_2O)_n^+$ ions fragment to lose at least one water molecule, even with two-color near-threshold ionization. An examination of the energetics of the observed fragmentation processes, including the strong binding of water molecules to $CH_2NH_2^+$ ions, will be presented elsewhere.[21]

Another interesting aspect of the clusters observed under jet expansion conditions is that more than one complex may be observed for a given host geometry, e.g., (PEAL **2**)W_1(a/b) and (PEA **3**)W_2(a/b). Their band origins have similar intensities (ca. 2:1), while their relative energies vary by a few kJ mol^{-1}, suggesting that the barriers to interconversion are great enough to prevent relaxation as these complexes cool in the jet. An effective "Boltzmann temperature" of a few hundred kelvin may be implied, although it is questionable whether the concept of equilibrium may be applied to complex formation in a jet expansion. Alternative 1:1 water complexes of tyramine have been observed previously,[9] although they were associated with binding to different functional groups (phenolic OH and alkyl NH_2).

Assignment of the PEA water cluster G to the structure (PEA **4**)W_1 has helped in the assignment of monomer feature D to PEA **4**. The structural differences between PEA **4** and PEA **5** were too small to allow their partially resolved band contours to be distinguished (A'' values differ by <1%). These changes were greatly amplified by the addition of a water molecule (A'' values differ by 20%), allowing the water cluster and by implication the nearby monomer feature to be assigned. In effect, the water molecule acts as a heavy atom tag in a fashion similar to argon.

It is noteworthy that the band contours analyzed in this study are all assigned to complexes in which primary hydrogen bonds are supplemented by additional stabilizing interactions. (PEAL **2**)W_1(b) benefits from an H$\cdots\pi$ interaction, with the water molecule placed over the ring in a manner very similar to benzene(H_2O). The resulting stabilization may be as much as 10 kJ mol^{-1}, the experimental binding energy in benzene-(H_2O).[16] The binding energy of a structure that places the water molecule in the plane of the benzene ring has been estimated to be only 60% as strong.[22] It is this $O_{water}\cdots HC_{ring}$ interaction that contributes to the additional stability of the complexes (PEA **3**)W_1(a) and (PEAL **2**)W_1(a). A similar interaction $O_{water}\cdots HC_{aliphatic}$ is found in the complex (PEA **4**)W_1(a). A neutron diffraction study of the crystal structures of carbohydrates, amino acids, and organometallic compounds containing water molecules found that O$\cdots$H$-$C bonds occur frequently and that CH donors tend to coordinate to water in concert with other hydrogen bonds.[23] The shortest O$\cdots$H bond distances were ca. 2.3 Å, but most were in the region 2.6$-$3.0 Å, similar to the distances calculated for PEA and PEAL clusters (ca. 2.7 Å).

In the context of this work, it is important to ask how well MP2/6-31G*//HF/6-31G* level calculations take account of these intermolecular interactions. First, we note that they are reflected in the HF optimized geometries; the water molecules are oriented in such a way to favor these interactions. The intermolecular bond lengths will no doubt change to some extent as optimization is carried out with larger basis sets and at higher

levels of theory, but for the purpose of supporting the present low-resolution work, it is unnecessary to obtain an extremely accurate set of rotational constants. The trends in binding energies at the MP2/6-31G*// HF/6-31G* level also reflect these interactions and appear to be in good accord with the experimental observations on PEA and PEAL clusters. The errors associated with incomplete basis sets are acceptable, since the experimental assignments do not rely too heavily on relative intensities. In some cases, however, relative energies have been used together with band contour appearance to aid the assignment of experimental bands. Comparison of simulated contours with PEA$(H_2O)_2$ band F and PEAL(H_2O) band C*, for example, did not allow unambiguous selection of a single ab initio structure. Of two possibilities, the more stable complex could be chosen in each case because the energy gap was so large (11 and 13 kJ mol^{-1}). A limitation that does arise is that complexes that vary *only in the orientation of the second unbonded hydrogen of water* cannot be distinguished because the differences in both relative energy and rotational constants are so small. Some of the structures shown in Figures 3−5 have slightly varying alternatives, but only one is presented, the structure with the (very slightly) greater binding energy (MP2/6-31G*//HF/6-31G*). The present experiments reveal the host structure and water binding sites, but fine details of bond lengths and accurate binding energies are not obtained. In this context, calculations using 6-31G* basis sets represent a reasonable compromise between computational effort and accuracy of the results.

Another result to come from this study is the extraordinary sensitivity of the $S_1 \leftarrow S_0$ TM alignments to the presence of water molecules. Previous work in this laboratory has shown that the sensitivity of the TM alignment to small structural changes may be used to distinguish individual conformers. That the same strategy may be applied to water clusters may be seen from Figure 3, for example. The influence of a water molecule on the TM alignment is quite strong in some cases. The experimental contour of PEA(H_2O) feature peak E, shown in Figure 7a, has a-type character, while the corresponding monomer feature, band C, is mostly b-type. This difference reflects a change in TM alignment in the molecular frame of at least 20°. The agreement with ab initio calculations at the CIS/6-31G* level is excellent. In the (PEA **3**)W_1(a) complex θ_{elec} is 43°, 21° greater than in PEA **3**, even though the distance $r_{O\cdots C(ring)}$ is 3.7 Å. A series of single-point CIS/6-31G* calculations were performed to investigate this enhanced TM rotation by modifying the complex in each of the following ways.

First, the water molecule was removed, leaving the PEA molecule in the geometry of the complex, giving $\theta_{elec}(1) = 28°$. Evidently, geometry changes induced in the PEA molecule by the water molecule have some effect. In particular, the change in the dihedral angle $C_2C_1C_\alpha C_\beta$ from 83° in the monomer to 80° in the complex is important because deviations in this angle away from 90° are strongly connected with TM rotations.[17] Second, the host molecule was rotated by 180° about an axis directed through the center of the ring and perpendicular to it, giving $\theta_{elec}(2) = 35°$. In effect, this placed the water molecule in an equivalent position on the opposite side of the ring, removing any contribution that might occur via the amine group. The result, when compared to the $\theta_{elec}(1)$, shows that there is clearly a "through-space" effect. Third, the water molecule was moved 60 pm further away from the ring by changing the dihedral angle CCNH(1) from 47° to 60°, while maintaining the same $r_{OH\cdots N}$ bond length, giving $\theta_{elec}(3) = 35°$. Since the water molecule has moved far enough from the ring to minimize direct through-space interactions, comparison with $\theta_{elec}(1)$ suggests that the water molecule has some effect acting through the hydrogen bond to the amine group. Last, the second (nonbonded) hydrogen atom H(2) of the water molecule was rotated about the O−H(1) bond in increments of 30°, to give values for θ_{elec} ranging from 14° when H(2) was directed toward the ring to 48° when the lone pair electron density of the oxygen was pointing toward the ring. This final result demonstrates how sensitive the TM alignment is to the orientation of the water molecule and suggests a significant "through-space" influence, even though the oxygen atom is located 3.7 Å from the nearest ring carbon atom.

It is important to gauge the reliability of CIS TM alignment predictions, since our strategy in assigning structures relies on a comparison of experimental band contours with simulations based on a range of different structural possibilities. $S_1 \leftarrow S_0$ TM alignments calculated using the CIS/6-31G* method are in excellent agreement with experimental results for a large number of substituted benzenes including PEA and PEAL,[6] methyl 3-hydroxybenzoate,[1] propylbenzene and butylbenzene,[4] 3-phenylpropionic acid and 3-(4-hydroxyphenyl)-propionic acid,[3] and tyrosol.[7] In a series of calculations on conformers of PEAL using the CI singles method with different basis sets, convergence of the TM alignment was achieved at the 6-31G level.[6] The present work allows some assessment of how reliable the TM predictions are for complexes where water molecules are in proximity to the ring. The CIS/6-31G* results are in excellent agreement with experimental results for the four hydrated PEA clusters but less convincing for those of PEAL. The predicted TM alignment of (PEAL **2**)W_1(b) is satisfactory, but the geometry of the complex in the S_1 state is uncertain. In the case of (PEAL **2**)W_1(a), θ_{elec} appears to be overpredicted by ca. 16°, which has a considerable effect on the appearance of the simulated contour. It is not clear why the TM alignment should be miscalculated for (PEAL **2**)W_1(a) when it appears to be accurate for (PEA **3**)W_1(a), a complex in which water binds in a very similar position. In summary, CIS predictions of $S_1 \leftarrow S_0$ TM alignments with 6-31G* basis sets are extremely useful, but some error may be introduced when solvent molecules are near the ring.

6. Conclusions

The combination of mass and spectral resolution and ab initio computation has proved to be a very effective strategy for the assignment of the hydrated clusters of PEA and PEAL produced in the low-temperature environment of a free jet expansion. This study demonstrates that even partially resolved band contours can reveal much about the binding of water molecules in moderately large systems. This is partly a result of the extraordinary sensitivity of the $S_1 \leftarrow S_0$ TM alignments of these molecules to small structural changes in the host and to the presence of water molecules. The ability to calculate ab initio a set of possible structures and to compare their predicted properties with experimental observations has been of crucial value and should find increasingly wide application.

Acknowledgment. We are grateful to the Leverhulme Trust for the provision of postdoctoral support (E.G.R.) and to the EPSRC for grant support and a studentship (M.R.H.). We thank the EPSRC Laser Support Facility for the loan of the GCR200/LAS laser system critical for the two-color experiments. We are especially grateful to Prof. John Simons for providing the inspiration and the resources for this work. We also thank Prof. Yehuda Haas, Dr Romano Kroemer, and Dr Michel Mons for helpful suggestions and stimulating discussions.

References and Notes

(1) Hepworth, P. A.; McCombie, J.; Simons, J. P.; Pfanstiel, J. F.; Riblett, J. W.; Pratt, D. W. *Chem. Phys. Lett.* **1995**, *236*, 571−579.

(2) Hepworth, P. A.; McCombie, J.; Simons, J. P.; Pfanstiel, J. F.; Ribblett, J. W.; Pratt, D. W. *Chem. Phys. Lett*. **1996**, *249*, 341−350.

(3) Dickinson, J. A.; Joireman, P. W.; Randall, R. W.; Robertson, E. G.; Simons, J. P. *J. Phys. Chem. A* **1997**, *101*, 513−521. Joireman, P. W.; Kroemer, R. T.; Pratt, D. W.; Simons, J. P. *J. Chem. Phys.* **1996**, *105*, 6075−6077.

(4) Dickinson, J. A.; Joireman, P. W.; Kroemer, R. T.; Robertson, E. G.; Simons, J. P. *J. Chem. Soc., Faraday Trans*. **1997**, *93*, 1467−1472.

(5) Elkes, J. M. F.; Robertson, E. G.; Simons, J. P.; McCombie, J.; Walker, M. *Phys. Chem. Commun*. **1998**, 1.

(6) Dickinson, J. A.; Hockridge, M. R.; Kroemer, R. T.; Robertson, E. G.; Simons, J. P.; McCombie, J.; Walker, M. *J. Am. Chem. Soc*. **1998**, *120*, 2622.

(7) Hockridge, M. R.; Knight, S. M.; Robertson, E. G.; Simons, J. P.; McCombie, J.; Walker, M. *PCCP* **1999**, *1*, 407.

(8) Sipior, J.; Teh, C. K.; Sulkes, M. *J. Fluoresc*. **1991**, *1*, 41−45.

(9) Teh, C. K.; Sulkes, M. *J. Chem. Phys*. **1991**, *94*, 5826.

(10) Martinez, S. J.; Alfano, J. C.; Levy, D. H. *J. Mol. Spectrosc*. **1993**, *158*, 82−92.

(11) Godfrey, P. D.; Hatherley, L. D.; Brown, R. D. *J. Am. Chem. Soc*. **1995**, *117*, 8204−8210.

(12) Sun, S.; Bernstein, E. R. *J. Am. Chem. Soc*. **1996**, *118*, 5086−5095.

(13) Gotch, A. J.; Zwier, T. S. *J. Chem. Phys*. **1992**, *96*, 3388.

(14) Lehrer, F. Ph.D. Thesis, Technical University of Munich.

(15) Chewter, L. A.; Sander, M.; Muller-Dethlefs, K.; Schlag, E. W. *J. Chem. Phys*. **1987**, *86*, 4737.

(16) Courty, A.; Mons, M.; Dimicoli, I.; Piuzzi, F.; Gaigeot, M.-P.; Brenner, V.; de Pujo, P.; Millié, P. *J. Phys. Chem. A* **1998**, *102*, 6590.

(17) Kroemer, R. T.; Liedl, K. R.; Dickinson, J. A.; Robertson, E. G.; Simons, J. P.; Borst, D. R.; Pratt, D. W. *J. Am. Chem. Soc*. **1998**, *120*, 12573.

(18) Frisch, M. J.; Trucks, G. W.; Schlegel, H. B.; Gill, P. M. W.; Johnson, B. G.; Robb, M. A.; Cheeseman, J. R.; Keith, T.; Petersson, G. A.; Montgomery, J. A.; Raghavachari, K.; Al-Laham, M. A.; Zakrzewski, V. G.; Ortiz, J. V.; Foresman, B.; Cioslowski, J.; Stefanov, B. B.; Nanayakkara, A.; Challacombe, M.; Peng, C. Y.; Ayala, P. Y.; Chen, W.; Wong, M. W.; Andres, J. L.; Replogle, E. S.; Gomperts, R.; Martin, R. L.; Fox, D. J.; Binkley, J. S.; Defrees, D. J.; Baker, J.; Stewart, J. P.; Head-Gordon, M.; Gonzalez, C.; Pople, J. A. *Gaussian 94*, revision C.3; Gaussian, Inc.: Pittsburgh, PA, 1995.

(19) Marten, B.; Kim, K.; Cortis, C.; Friesner, R. A.; Murphy, R. B.; Ringnalda, M. N.; Sitkoff, D.; Honig, B. *J. Phys. Chem.* **1996**, *100*, 11780.

(20) Fowler, J. E.; Schaefer, H. F. *J. Am. Chem. Soc*. **1995**, *117*, 446.

(21) Hockridge, M. R.; Robertson, E. G.; Haas, Y. Manuscript in preparation.

(22) Karlstrom, G.; Linse, P.; Wallqvist, A.; Jonsson, B. *J. Am. Chem. Soc*. **1983**, *105*, 3777.

(23) Steiner, T.; Saenger, W. *J. Am. Chem. Soc*. **1993**, *115*, 4540.